Electronic Supplementary Material (ESI) for Journal of Materials Chemistry A.
This journal is © The Royal Society of Chemistry 2018

Creating Ultrathin Amorphous Metal Hydroxide and Oxide nanosheets Libraries

BinbinJia, [a]RuiHao, [a]Zhongning Huang, [a]Pengfei Hu, [a]Lidong Li, *[a] YanZhang[a] and Lin Guo*[a]

a. Key Laboratory of Bio-inspired Smart Interfacial Science and Technology ofMinistryofEducation, Beijing Advanced Innovation Center for Biomedical Engineering, School of Chemistry,Beihang University, Beijing 100191, P. R. China.

Experimental Section

Synthesis of Cu_2O ultrathin nanosheets. Preparation of lamellar Cu_2O-oleate complex intermediate: The lamellar Cu_2O-oleate complex intermediate was synthesized by a hydrothermal method. In a typical procedure, 99 mg CuCl, 914 mg sodium oleate, 831 mg hexamethylenetetramine (HMT) and 100 μL $N_2H_4{\cdot}H_2O$ were added into 40 mL distilled water orderly. After vigorous stirring for 10 min, the mixed solution was transferred into 50 mL teflon cup and heated in a sealed autoclave at 100 °C for 24 h. Upon cooling to room temperature naturally, the final product was collected by centrifuging the mixture, washed with distilled water and absolute ethanol for several times, and then dried in vacuum at 60 °C overnight for further analysis.50 mg lamellar Cu_2O-oleate complex intermediate was put in a quartz boat and then heated at 300 °C for 8 min in air, then the sample was allowed to cool down to room temperature naturally. The Cu_2O colloidal solution was achieved by dispersing 20 mg calcined product into 10 mL absolute ethanol by ultrasonic for 40 min. The final product was collected by centrifuging the supernatant at 12,000 rpm for 10 min, and then dried in vacuum overnight for further characterization.

Synthesis of amorphous $Co(OH)_2$ ultrathin nanosheets. In a typical synthesis, 5 mg Cu_2O nanosheets and 2 mg $CoCl_2{\cdot}5H_2O$ were dissolved in mixed solutions including 10 ml deionized water and 10 ml ethanol. And then, the $Na_2S_2O_3$ solution (0.4 m 10 ml) was slowly added to the mixed solutions through a constant pressure titration funnel maintained at 20 ℃ for 1 h. The precipitate was collected after centrifugation and carefully washed with water and ethanol to clean out remnant salt and dried in vacuum overnight for further characterization.

Synthesis of amorphous CoO ultrathin nanosheets. The dried amorphous $Co(OH)_2$ nanosheets products were under thermo treatment at 250 ℃ for 1 hours in argon atmosphere, during which the heating rate was 5℃/min.

Synthesis of amorphous $Zn(OH)_2$ ultrathin nanosheets.In a typical synthesis, 5 mg Cu_2O nanosheets and 3 mg $ZnCl_2$ were dissolved in mixed solutions including 10 ml deionized water and 10 ml ethanol. And then, the $Na_2S_2O_3$ solution (0.4 m 10 ml) was slowly added to the mixed solutions through a constant pressure titration funnel maintained at 20 ℃ for 1 h. The precipitate was collected after centrifugation and carefully washed with water and ethanol to clean out remnant salt and subsequently dried in vacuum overnight for further characterization.

Synthesis of amorphous ZnO ultrathin nanosheets. The dried amorphous $Zn(OH)_2$ nanosheets products were under thermo treatment at 250 ℃ for 1 hours in argon atmosphere, during which the heating rate was 5℃/min.

Synthesis of amorphous $Mg(OH)_2$ ultrathin nanosheets. In a typical synthesis, 5 mg Cu_2O nanosheets and 1.7 mg $MgCl_2$ were dissolved in mixed solutions including 10 ml deionized water and 10 ml ethanol. And then, the $Na_2S_2O_3$ solution (0.4 m 10 ml) was slowly added to the mixed solutions through a constant pressure titration funnel maintained at 20 ℃ for 1 h. The precipitate was collected after centrifugation and carefully washed with water and ethanol to clean out remnant salt and subsequently dried in vacuum overnight for further characterization.

Synthesis of amorphous MgO ultrathin nanosheets.The dried amorphous $Mg(OH)_2$ nanosheets products were treated with calcination at 250 ℃ for 1 hours in argon atmosphere and the heating rate was 5℃/min.

Synthesis of amorphous $Mn(OH)_x$ ultrathin nanosheets. In a typical synthesis, 5 mg Cu_2O nanosheets and 2.5 mg $MnCl_2{\cdot}2H_2O$ were dissolved in mixed solutions including 10 ml deionized water and 10 ml ethanol. And then, the $Na_2S_2O_3$ solution (0.4 m 10 ml) was slowly added to the mixed solutions through a constant pressure titration funnel maintained at 20 ℃ for 1 h. The precipitate was collected after centrifugation and carefully washed with water and ethanol to clean out remnant salt and subsequently dried in vacuum overnight for further characterization.

Synthesis of amorphous MnO_x ultrathin nanosheets. The dried amorphous $Mn(OH)_x$ nanosheets products were treated with calcination at 250 ℃ for 1 hours in argon atmosphere, duing which the heating rate was 5℃/min.

Synthesis of amorphous $Fe(OH)_3$ ultrathin nanosheets. In a typical synthesis, 5 mg Cu_2O nanosheets and 1.3 mg $FeCl_2{\cdot}4H_2O$ were dissolved in 20 ml deionized water. And then, the $Na_2S_2O_3$ solution (0.2 m 10 ml) was slowly added to the mixed solutions through a constant pressure titration funnel maintained at 20 ℃ for 1 h. The precipitate was collected after centrifugation and carefully washed with water and ethanol to clean out remnant salt and subsequently dried in vacuum overnight for further characterization.

Synthesis of amorphous Fe_2O_3 ultrathin nanosheets. The dried amorphous $Fe(OH)_3$ nanosheets products were under thermo treatment at 250 ℃ for 1 hours in a argon atmosphere, during which the heating rate was 5 ℃/min.

Material Characterizations. The morphology of amorphous nanosheets were characterized with a scanning electron microscopy (7500F, JEOL). The transmission electron microscopy (TEM) images were obtained with JEOL JEM- 2100F at an accelerating voltage of 200 kV. Atomic force microscope (AFM) were performed by a Bruker Dimension Icon and the samples were dispersed on mica plate.

*Electrochemical Tests.*The catalysts (1 mg) were dispersed in solvent consisted of 350 μL of deionized water, 135 μL of alcohol and 15 μL of 5 wt% Nafion solution. After sonication for 15 min, 20 μL of homogeneous solution was drop onto glassy carbon electrode. The fabrication of working electrodes was finished,after drying at room temperature. Electrochemical Tests were performed in a standard three-electrode system controlled by Pine Instruments electrochemistry workstation. Pt wire work as a counter electrode and Ag/AgCl electrode work as the reference electrode. All potentials measured were calibrated to the reversible hydrogen electrode (RHE) using the following equation: ERHE = EAg/AgCl + 0.197 V +0.059 pH, where pH = 14 in 1 M KOH solution. To get rid of the generated oxygen bubbles, working electrode should be rotated at 1600 rpm. In addition, LSVs were performed at 2 mV s^{-1} for polarization curves and Tafel plots should be tested at the scan rate of0.1 mV s^{-1} .

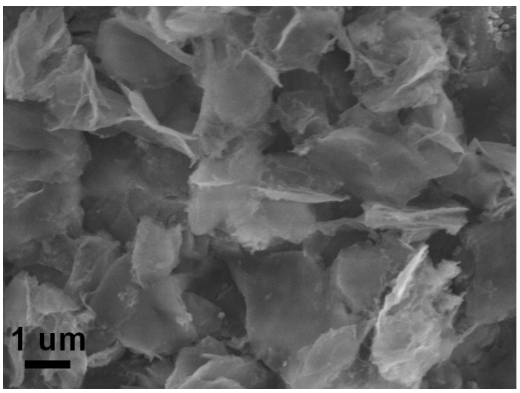

Figure S1.SEM images of Cu_2O nanosheets.

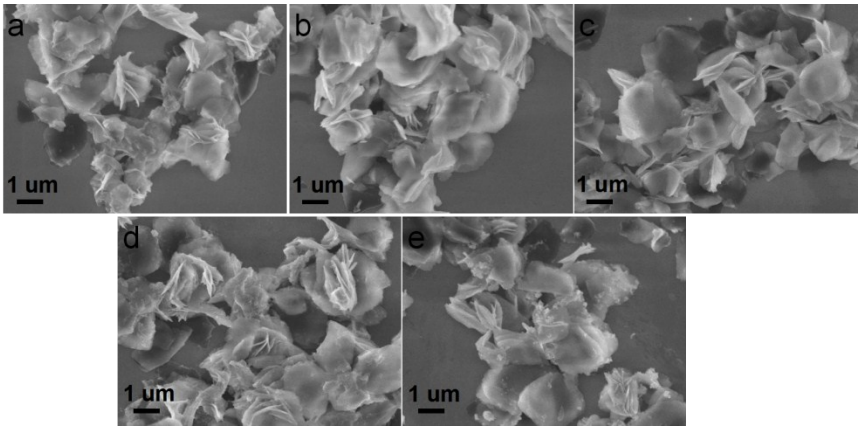

Figure S2. SEM images of amorphous metal hydroxide nanosheets (a) $Co(OH)_2$, (b) $Mg(OH)_2$, (c) $Zn(OH)_2$, (d) $Mn(OH)_x$, (e) $Fe(OH)_3$.

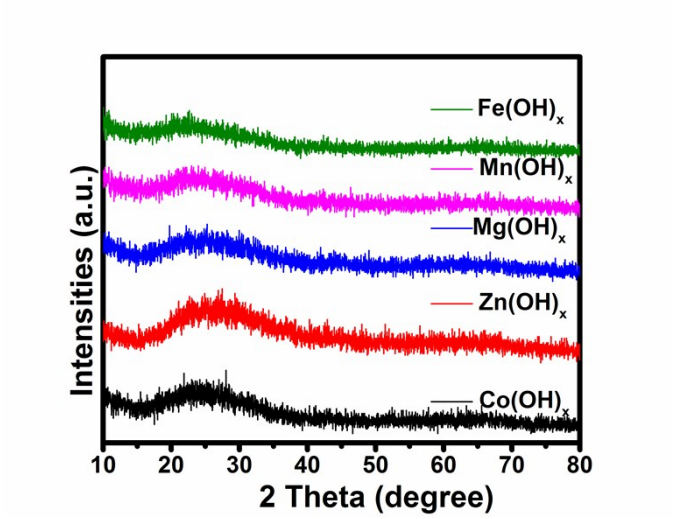

Figure S3.XRD patterns of metal hydroxide nanosheets.

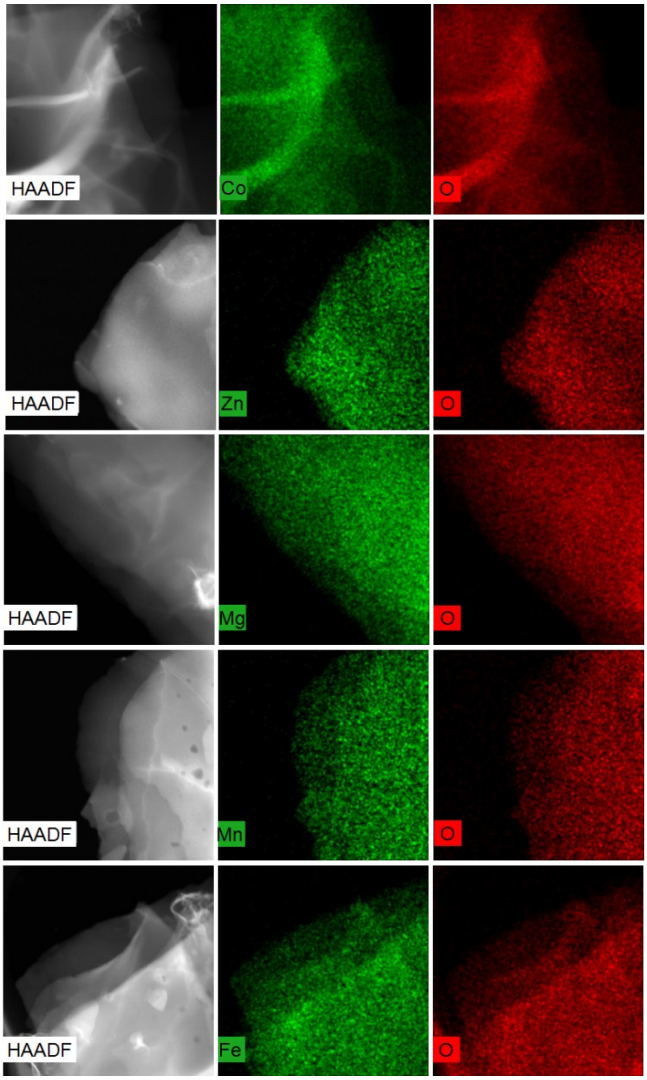

Figure S4. Elemental mapping imagesof amorphous metal hydroxide nanosheets.

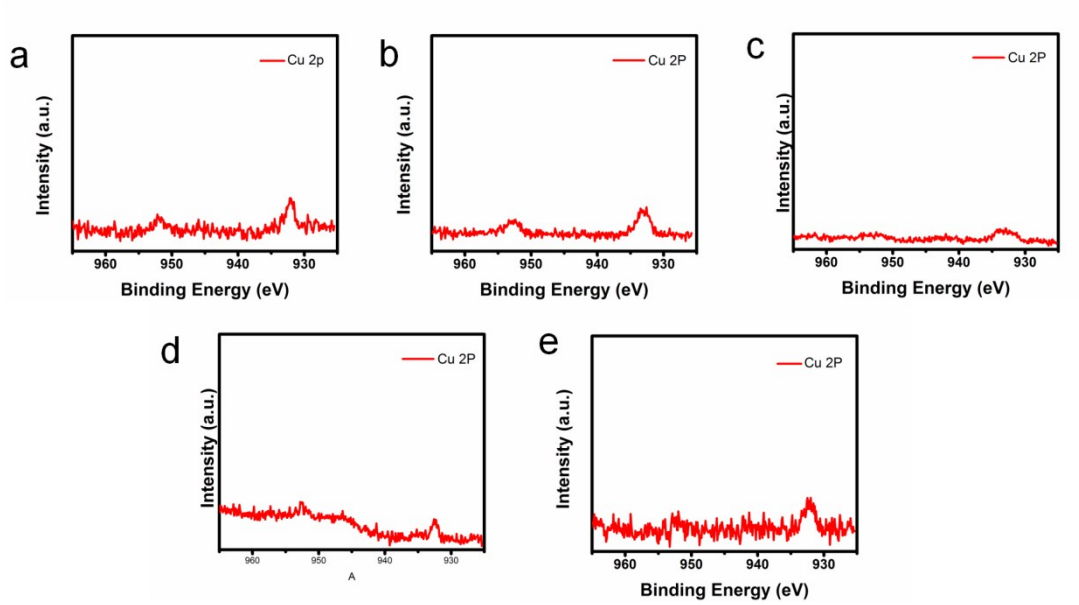

Fig. S5. The XPS spectra of Cu 2p in the amorphous $M(OH)_x$ nanosheets, (a) $Co(OH)_2$ (b) $Zn(OH)_2$, (c) $Mg(OH)_2$, (d)$MnOH_2$/MnOOH, and (e) $Fe(OH)_3$.

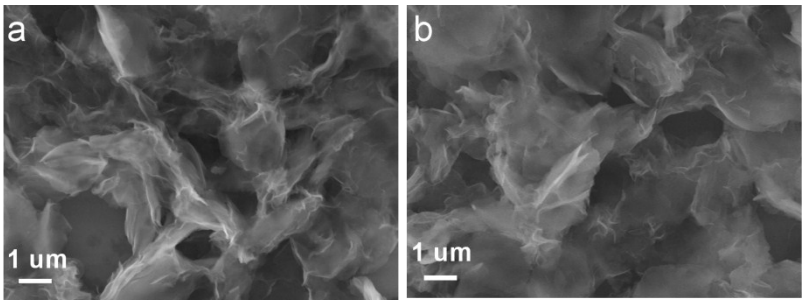

Figure S6. SEM images of different atomic ratios of amorphous $Co_xZn_y(OH)_w$ nanosheets.

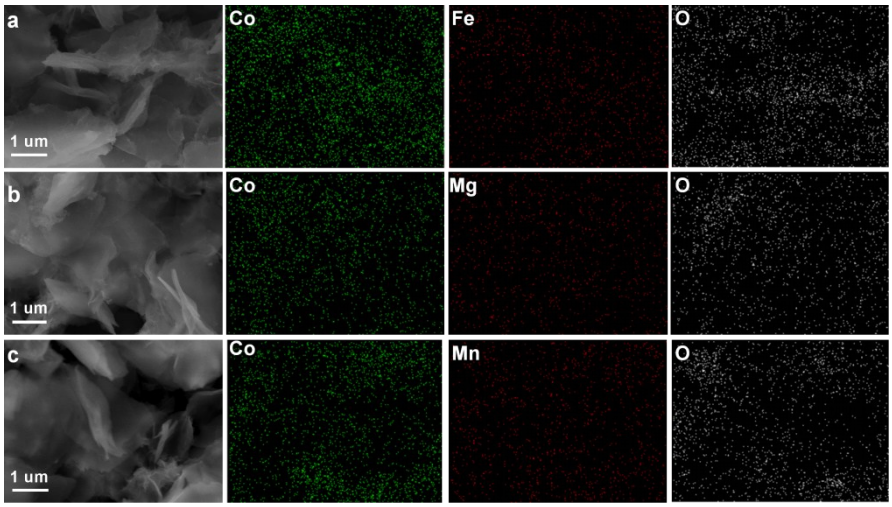

Figure S7. SEM images and elemental mapping images of (a) amorphous $Co_xFe_y(OH)_w$ nanosheet, (b) $Co_xMg_y(OH)_w$ nanosheet, and $Co_xMn_y(OH)_w$ nanosheet.

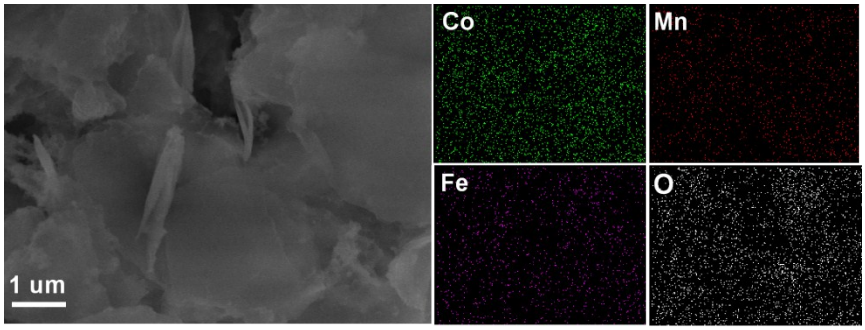

Figure S8. SEM image and elemental mapping images of amorphous $Co_xMn_yFe_z(OH)_w$ nanosheet.

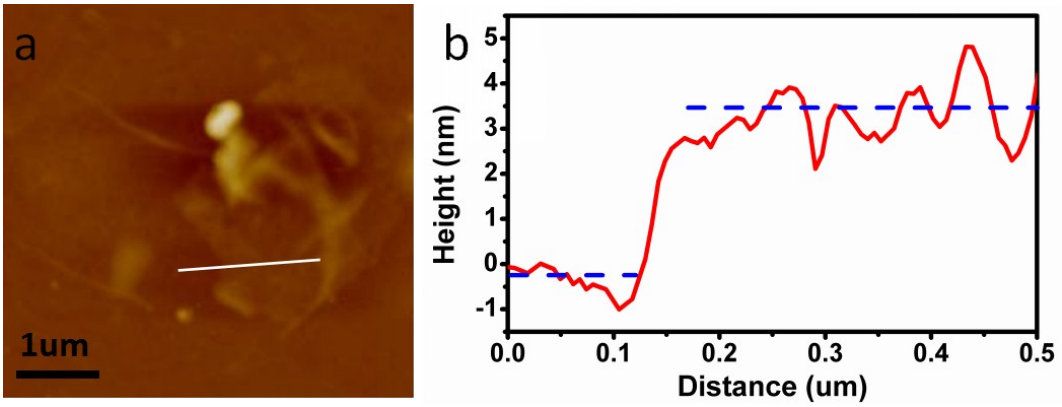

Figure S9. The AFM image (a) and AFM height image (b) of ta-$Co(OH)_2$ nanosheets.

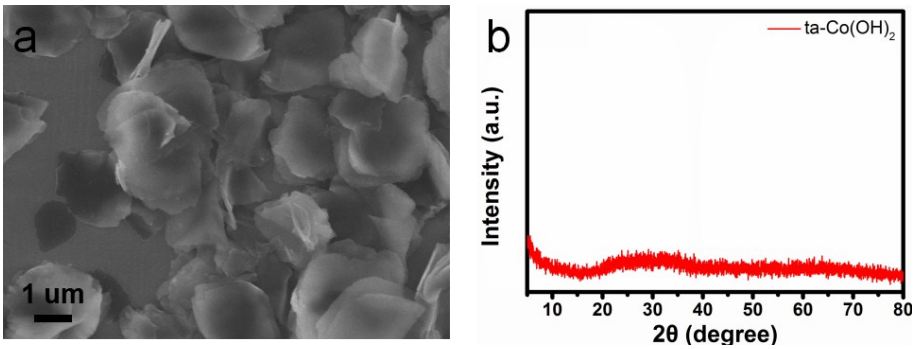

Figure S10. The SEM image (a) and XRD patterns (b) of ta-$Co(OH)_2$.

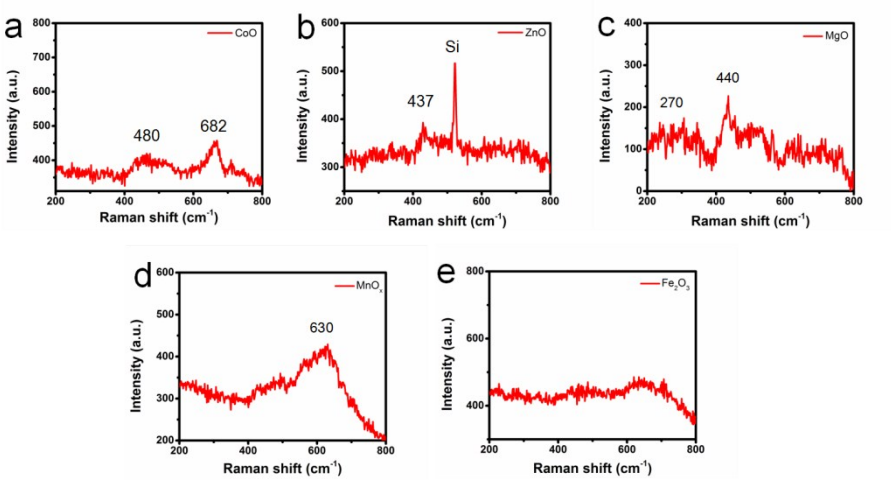

Figure S11. Raman spectra of metal oxide nanosheets.

Raman spectra of amorphous metal oxide nanosheets were also conducted in the range of 200-800 cm^{-1}. As shown in Figure S11. The Raman peaks of amorphous MO_x become wider and weaker compared to corresponding crystalline MO_x. The Raman spectrum of annealed cobalt oxide is shown in FigureS15a. The peaks at 480 and 682 cm^{-1} are the characteristic peaks for CoO.[1] Figure S15b shows a typical Raman scattering spectrum of amorphous ZnO. The peak at 437 cm^{-1} can be assigned to E_2 mode of ZnO, while the peak at 580 cm^{-1} is not detected.[2] The Raman spectrum of amorphous MgO is shown in Figure S15c. The peaks at 270 cm^{-1} and 440 cm^{-1} are similar to the previous report for MgO.[3] Figure S15d shows a typical Raman scattering spectrum of amorphous MnO_x. In particular, the peak centered at 630 cm^{-1} is characteristic of the Mn_2O_3 species. Due to the wider width of the main peak, the peak at 580 cm^{-1} is encapsulated.[4] Combining with the corresponding hydroxide nanosheets, the sample should be a mixture of MnO and Mn_2O_3 (termed MnO_x). For amorphous Fe_2O_3, the absorption bands in the range 200-800 cm^{-1}, which are characteristic of the Fe-O vibration mode, are present in all the samples. The Raman spectrum of the sampleis similar to the previous reports of the maghemite material.[5]

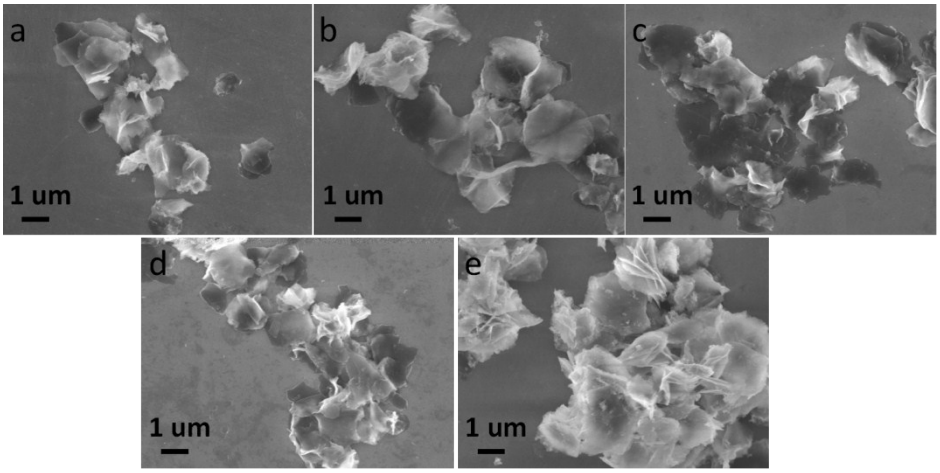

Figure S12. SEM images of amorphous metal oxide nanosheets (a) CoO, (b) MgO, (c) ZnO, (d) MnO_x, (e) Fe_2O_3.

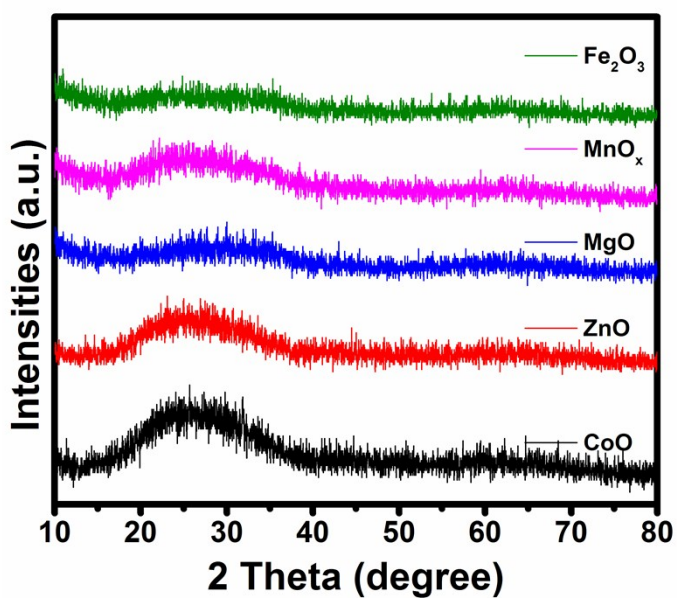

Figure S13. XRD patterns of metal oxide nanosheets.

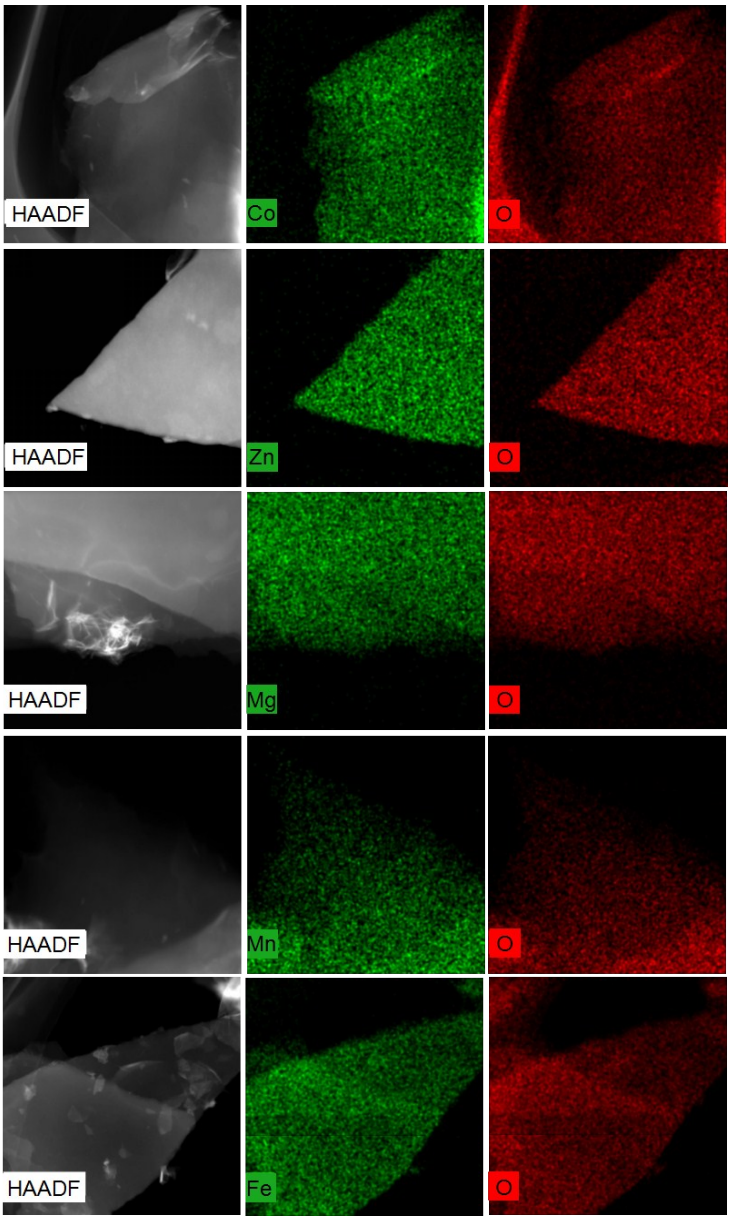

Figure S14. Elemental mapping images of amorphous metal oxide nanosheets.

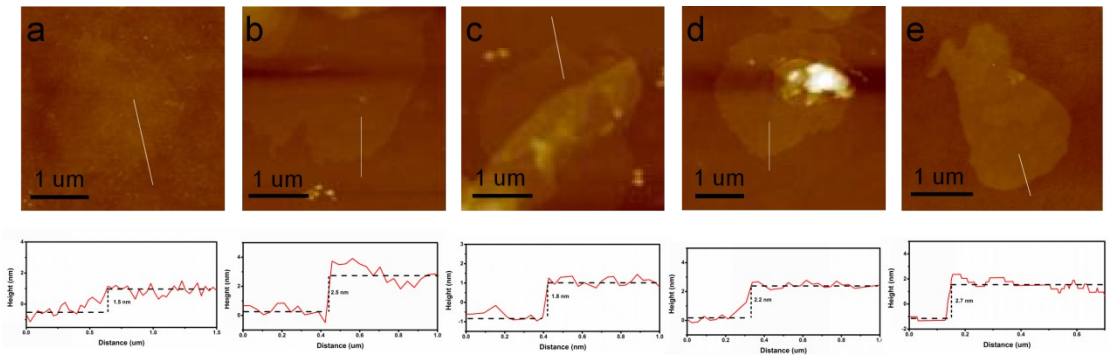

Figure S15. The AFM images and AFM height images of amorphous metal oxide nanosheets ((a) CoO, (b) ZnO, (c) MgO, (d) MnO_x, (e) Fe_2O_3), respectively.

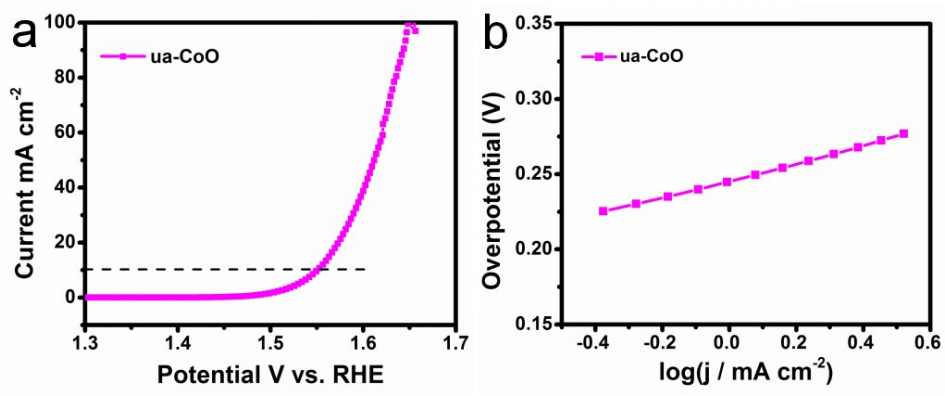

Figure S16. The OER activity of amorphous CoO nanosheets after calcination. (a) LSV curves (b) Tafel plots of amorphous CoO nanosheets.

Table S1. The Ksp and pKsp of amorphous metal hydroxide nanosheets.

sample	K_{sp}	pK_{sp}
$Co(OH)_2$	5.92×10^{-15}	14.23
$Zn(OH)_2$	3×10^{-17}	16.5
$Mg(OH)_2$	1.8×10^{-11}	10.74
$Mn(OH)_2$	1.9×10^{-13}	12.72
$Fe(OH)_2$	4.87×10^{-17}	16.31

Table S2. The thickness of amorphous metal hydroxide nanosheets.

sample	$Co(OH)_2$	$Zn(OH)_2$	$Mg(OH)_2$	$Mn(OH)_x$	$Fe(OH)_3$
thickness (nm)	1.4	2.4	1.6	1.9	2.7

Table S3. The atomic ratio of M and Cu tested by ICP.

sample	Atomic %(M)	Atomic % (Cu)
$Co(OH)_2$	92.6	7.4
$Zn(OH)_2$	93.4	6.6
$Mg(OH)_2$	97.2	2.8
$Mn(OH)_x$	98.2	2
$Fe(OH)_3$	96.5	3.5

Table S4. The thickness of amorphous metal hydroxide nanosheets.

sample	CoO	ZnO	MgO	MnO_x	Fe_2O_3
thickness (nm)	1.2	2.5	1.8	2.2	2.7

Table S5. Comparison of the amorphous $Co(OH)_2$ catalysts with recentlyreported Co-based catalysts.

catalysts	η (10mA cm^{-2}) (V)	Tafel slope (mV dec^{-1})	references
ua-$Co(OH)_2$ nanosheet	0.267	34.4	Our work
Gelled-FeCoW	0.223	37	Ref. 6
Co(OH)F	0.313	53	Ref. 7
CoOOH nanosheets	0.3	38	Ref. 8
CoMn LDH	0.324	43	Ref. 9
plasma-engraved Co_3O_4 nanosheets	0.3	68	Ref. 10
$Co(SxSe_{1-x})_2$ Nanoparticles	0.283	65.6	Ref. 11
$Fe_{0.33}$ $Co_{0.67}$ OOH	0.266	30	Ref. 12
Amorphous $Co(OH)_2$	0.36	56	Ref. 13
α-$Co(OH)_2$ nanosheets	0.317	49	Ref. 14
$Ni_{0.6}Co_{1.4}P$ Nanocages	0.3	80	Ref. 15

References

1 S. G. Kandalkar, C.D. Lokhande, R.S.Mane and S. H. Han, Appl. Surf. Sci., 2007, **253**, 3952.
2 Z.J. Wang, H. M. Zhang, Z. J. Wang, L. G. Zhang, J. S. Yuan, S. G. Yan and C.Y. Wang, J. Mater. Res., 2003, **18**, 151.
3 T. S. Duffy , C. Meade, Y. W. Fei, H. K. Mao and R. J. Hemley, Am. Mineral, 1995, **80**, 222.
4 Y. T. Hu and J. Wang, J. Power Sources, 2015, **286**, 394.
5 Y. L. Zheng, W. Z. Wang, D. Jiang and L. Zhang, Chem. Eng. J., 2016, **284**, 21
6 B. Zhang, X. L. Zheng, O. Voznyy, R. Comin, M. Bajdich, M. Garcia-Melchor, L. L. Han, J. X. Xu, M. Liu, L. R. Zheng, F. P. G. de Arquer, C. T. Dinh, F. J. Fan, M. J. Yuan, E. Yassitepe, N. Chen, T. Regier, P. F. Liu, Y. H. Li, P. De Luna, A. Janmohamed, H. L. L. Xin, H. G. Yang, A. Vojvodic and E. H. Sargent, *Science*, 2016, **352**, 333.
7 S. Wan, J. Qi, W. Zhang, W. Wang, S. Zhang, K. Liu, H. Zheng, J. Sun, S. Wang and R. Cao, *Adv. Mater.*, 2017, **29**, 1700286.
8 J. H. Huang, J. T. Chen, T. Yao, J. F. He, S. Jiang, Z. H. Sun, Q. H. Liu, W. R. Cheng, F. C. Hu, Y. Jiang, Z. Y. Pan and S. Q. Wei, *Angew. Chem. Int. Ed.*, 2015, **54**, 8722.
9 F. Song and X. L. Hu, *J. Am. Chem. Soc.*, 2014, **136**, 16481.
10 L. Xu, Q. Q. Jiang, Z. H. Xiao, X. Y. Li, J. Huo, S. Y. Wang and L. M. Dai, *Angew. Chem. Int. Ed.*, 2016, **55**, 5277.
11 L. Fang, W. X. Li, Y. X. Guan, Y. Y. Feng, H. J. Zhang, S. L. Wang and Y. Wang, *Adv. Funct. Mater.*, 2017, **27**, 1701008.
12 S. H. Ye, Z. X. Shi, J. X. Feng, Y. X. Tong and G. R. Li, *Angew. Chem. Int. Ed.*, 2018, **57**, 2672.
13 M. Abu Sayeed, T. Herd and A. P. O'Mullane, *J. Mater. Chem. A.*, 2016, **4**, 991.
14 Y. M. Jiang, X. Li, T. X. Wang and C. M. Wang, *Nanoscale*, 2016, **8**, 9667.
15 B. C. Qiu, L. J. Cai, Y. Wang, Z. Y. Lin, Y. P. Zuo, M. Y. Wang and Y. Chai, *Adv. Funct. Mater.*, 2018, **28**. 1706008.